An ALS Assembly Modulator Signature in Peripheral Blood Mononuclear Cells: Implications for ALS Pathophysiology, Therapeutics, and Diagnostics

Shao Feng Yu[1], Maya Michon[1], Anuradha F. Lingappa[1], Kumar Paulvannan[1], Dennis Solas[1], Kim Staats[2], Justin Ichida[2], Debendranath Dey[1], Jeffrey Rosenfeld[3] and Vishwanath R. Lingappa[1,4,5]

[1] Prosetta Biosciences, Inc. 670 5th St San Francisco, CA 94107

[2] University of Southern California, Los Angeles, CA 90033

[3] Loma Linda Medical Center, Loma Linda, CA 92354

[4] Department of Physiology, University of California, San Francisco, CA 94143

[5] To whom correspondence should be directed (vlingappa@prosetta.com)

Abstract

Assembly modulators are a new class of allosteric site-targeted therapeutic small molecules, some of which are effective at restoring nuclear localization of TDP-43 in ALS cellular models, and which display efficacy in a variety of ALS animal models. These compounds have been shown to bind selectively to a small subset of protein disulfide isomerase (PDI), a protein implicated in ALS pathophysiology. The targeted subset of PDI is found within a novel, transient and energy-dependent multi-protein complex that includes other important members of the ALS interactome, such as TDP-43, RanGTPase, and selective autophagy receptor p62/SQSTM1. We demonstrate here that a similar multi-protein complex drug target is present in PBMCs as isolated by energy-dependent drug resin affinity chromatography (eDRAC) and characterized by mass spectrometry and by Western blot (WB). Signature alterations in the composition of the multi-protein complex in PBMCs from ALS patients compared to PBMCs from healthy individuals were identified by WB of eDRAC free drug eluates, thereby extending earlier literature suggesting PBMC dysfunction in ALS. Changes in the PBMC drug target in ALS patients compared to healthy individuals include diminished p62/SQSTM1 and appearance of a 17kDa post-translationally modified form of RanGTPase. These changes are not readily apparent from analysis of whole cell extracts, as the individual protein components within the drug target multi-protein complex comprise only miniscule percentages of the total of the component proteins in the extract. Furthermore, whole blood from ALS patients shows a distinctive degradation of RanGTPase not observed in blood from healthy individuals. This degradation appears to be rescued by treatment of whole blood from ALS patients for 72 hrs with ALS-active assembly modulator small molecules. Our findings are consistent with the hypothesis that ALS is

45 fundamentally a disorder of homeostasis that can be detected early, prior to disability, in blood
46 and restored to the healthy state by assembly modulator treatment.
47
48 **Introduction**
49 Amyotrophic Lateral Sclerosis (ALS) is a devastating neurodegenerative disease that
50 strikes approximately 6,000 American and 150,000 people worldwide annually[1,2]. Approximately
51 10% of ALS is familial, with a large number of specific gene mutations implicated. The vast
52 majority of ALS cases however, are sporadic, meaning that that there is no family history of the
53 disease and therefore seems likely due to an environmental cause, perhaps with epigenetic
54 influence[3]. Specific environmental factors have been implicated in causing ALS, but remain
55 controversial and inconclusive[4]. While the pathophysiology of ALS is not well understood,
56 aggregates of the protein TDP-43, independently implicated in the HIV life cycle[5], are almost
57 invariably found in the brains of patients with ALS and fronto-temporal dementia (FTD)[6].
58 Despite this commonality, the clinical presentation as well as progression of ALS, is highly
59 variable[7].
60
61 With regards to TDP-43 pathophysiology, controversy exists as to the triggering event.
62 Some studies have implicated mislocalization of TDP-43 from the nucleus in healthy cells to the
63 cytoplasm, which is observed to variable degrees in fibroblasts from many, but not all, cases of
64 ALS[8]. An alternative view is that, in response to stress, TDP-43 forms aggregates in the
65 cytoplasm where it is synthesized, prior to transport to the nucleus[9]. A further controversy
66 exists as to whether the relevant TDP-43 aggregates in the cytoplasm are within, or outside of,

67 stress granules[10]. While the TDP-43 aggregates have generally been viewed as a trigger of motor
68 neuron death, it is possible that they are an epiphenomenon whose elimination *per se* may not
69 necessarily be therapeutic, by analogy to the failed attempts to remedy Alzheimer's Disease by
70 elimination of Aβ aggregates[11]. Regardless of their natural history and role in the
71 pathophysiology of ALS, the presence of TDP-43 aggregates are pathognomonic for the
72 disease[12,13].
73
74 Recently we presented our studies on the role of a newly appreciated dimension of gene
75 expression, termed protein assembly, in the pathophysiology of diverse diseases including
76 ALS[14,15,16]. These compounds were found by a novel method in which viruses were used as
77 "trufflehounds" to reveal drug targets inaccessible by genomic or conventional proteomics[15,16].
78 We have identified several structurally unrelated small molecule chemotypes by virtue of their
79 ability to modulate host machinery catalytic for viral capsid formation, that we term protein
80 assembly modulators. These compounds are strikingly efficacious both for the specific viral
81 disease by which they were identified and also for a subset of non-viral diseases. Among the
82 protein assembly modulators with activity against HIV, are a subset that prevent ALS-associated
83 neurodegeneration and its correlates in various cellular and animal models of ALS[14]. The
84 compounds are broadly effective at reversing both TDP-43 mislocalization and stress-induced
85 TDP-43 aggregation, in both familial and sporadic ALS and fronto-temporal dementia (FTD)
86 cellular models. Efficacy has also been demonstrated in various transgenic animals expressing
87 human ALS-causing mutations including in TDP-43, FUS, c9orf72, and SOD1, by a variety of
88 assays[14]. In view of this breadth of efficacy, we hypothesized the drug target to be a step

common to most, if not all, ALS and FTD. Advanced analogs of an ALS-selective active subseries of one of these chemotypes are close to completion of a target product profile (TPP), prior to initiation of investigational new drug (IND)-enabling studies in anticipation of human clinical trials in the near future.

The studies to be described here had several motivations. First, to explore the hypothesis that the biochemical pathways involved in ALS pathophysiology may involve layers of regulation yet to be discovered[17,18], in which the novel multi-protein complex targets of these compounds might be involved. How those levels of control are integrated with one another, and are communicated from one organ system to others, remain largely unknown. It may be that the novel assembly modulator targets we have discovered are potential candidates for involvement in such regulation. By corollary, what happens to other feedback controls when one level of regulation fails, remains to be determined. The argument has been made based on gene knockout experiments that more ancient back up pathways may be activated when primary regulatory controls fail[19,20]. Having a drug that impinges on a biochemical pathway in a novel way is a powerful means of probing biological regulation. Much of this regulation depends on information that does not reside simply in the sequence of the genome[18,20,21]. Thus the relevance of the compounds we describe, with their unconventional multi-protein complex target (energy-dependent for formation, transient in existence, composed of miniscule subsets of the individual component proteins in the cell), and novel mechanism of action at allosteric sites[22,23 24,25]. These tools may provide a new understanding of the molecular basis for homeostasis, and its dysregulation, as exemplified in ALS.

111

112 A second motivation for the present studies was to understand the meaning of the
113 observed dysfunction of PBMCs in ALS[26,27]. These findings can be interpreted in very different
114 ways. On the one hand, PBMC dysfunction might be due to ALS being a systemic disease whose
115 most severe manifestation is motor neuron death, but which also manifests in less dramatic
116 fashion in other organ systems, including in blood. Alternatively, the signature observed in
117 PBMCs might reflect a role of blood, which sees essentially every cell in the body on a regular
118 basis, spreading the message that there is a disorder affecting a particular cell type, in this case,
119 motor neurons. Yet another possibility is that the disorder affecting one organ system (motor
120 neurons) could have a "domino effect" manifesting in other organ systems (PBMCs), e.g. as a
121 secondary consequence of feedback regulation intended to monitor and maintain
122 homeostasis[17,28]. Prion-type spread of various diseases may be an example of such disordered
123 communication[28–30]. Towards this end, we asked whether assembly modulator drugs might also
124 detect a version of the disordered drug target in PBMCs from ALS patients.

125

126 Finally, apart from intellectually interesting questions of feedback and mechanism of
127 action[17,28,30], there is a practical desire to advance these compounds to the clinic, given their
128 remarkable therapeutic properties in cellular and animal models of ALS[31]. Having a readily
129 accessible signature of ALS in PBMCs would facilitate ALS drug advancement in innumerable
130 ways, most importantly by making possible early detection of ALS (prior to severe disability).
131 Compounds designed to restore homeostasis would be expected to be most effective when
132 administered early, before motor neuron death. Or put another way, treatments that restore

133 homeostasis would be expected to be very different from those needed to regrow and replace
134 cells that have died. A signature in PBMCs would also provide a biomarker for easy assessment
135 of therapeutic efficacy and when therapy could be stopped or might need to be restarted.
136
137 **Results**
138 Blinded blood samples were obtained from ALS patients and healthy individuals, under
139 an IRB-approved protocol. The PBMCs were isolated, and extracts prepared as described in
140 methods, and analyzed for key proteins relevant to ALS. Differences observed in the protein
141 pattern between PBMCs of healthy and ALS patients, by total protein silver stain were subtle
142 (see for example, **Figure 1A**).
143 However when PBMC extracts were applied to the ALS-active drug resin described
144 previously[31] versus control resin (lacking the drug ligand), washed and bound material analyzed,
145 a distinctive subset of proteins was observed, also largely shared between healthy individuals
146 and ALS patients, but with a few possible differences (black arrows in **Figure 1B**).
147 Previous studies of assembly modulator small molecules[15,16] have shown that the
148 proteins comprising the multi-protein complex drug target represent single digit percent of the
149 total of those proteins in the starting extract. As expected therefore, the depleted extracts differ
150 very subtly from the starting material, as demonstrated for PBMC DRAC flow through here (see
151 Supplemental Figure 1).

Figure 1

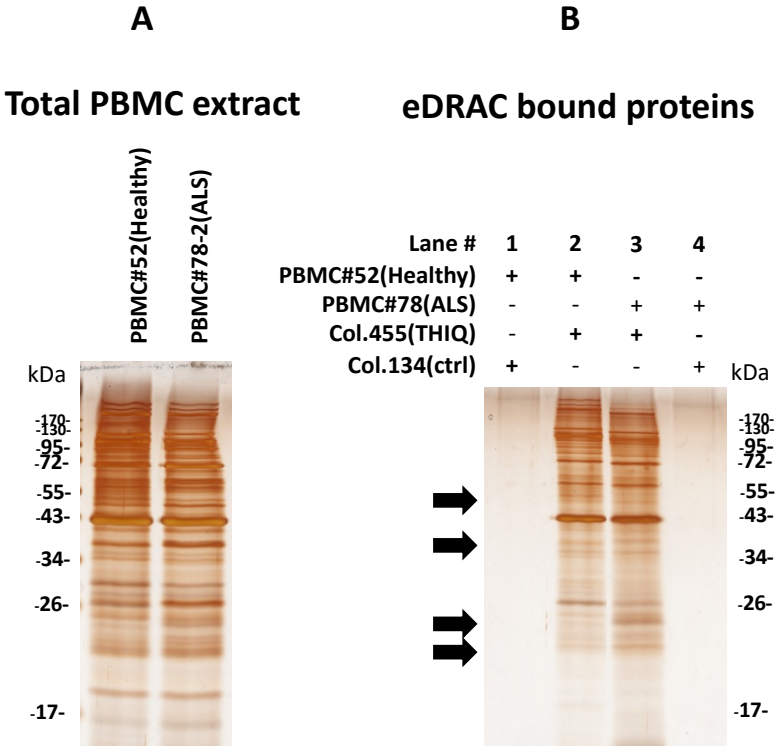

Legend to Figure 1. A. Silver stain of starting PBMC extract 10kxg/10min supernatant from a representative healthy individual (#52) and an ALS patient (#78-2). B. Silver stain of free drug eluate from ALS-active assembly modulator drug resin (column 455 THIQ) or control resin (column 134 lacking the drug ligand). Black arrows indicate positions at which healthy vs ALS patient samples show a suggestive difference in the free drug eluate protein pattern.

Mass spectrometry analysis of free drug eluates from PBMCs applied to the ALS-active drug resin (**Figure 2**) was carried out and compared to the pattern previous revealed from mouse brain (MoBr). A substantial proportion of tissue-specific proteins (~1/2 to 2/3 depending on the specific sample) were observed (see **Supplemental Figure 2**). Despite the high tissue specificity, a core set of 33 proteins shared between both PBMCs and brain were of interest. Of these, 26 were identified as members of the ALS protein interactome. Notably, this set included P4HB, a

member of the PDI family, two known ALS-causing proteins (TUBA4A and VCP)[32], along with proteins implicated in the KEGG ALS interactome[33] (ATP5A1, HSPA5, TUBA1A, TUBA4A, and VCP). Furthermore, 24 of these 33 proteins exhibited high-confidence interactions with known ALS-causing or disease-modifying proteins[32]. The 26 shared ALS interactome proteins also included multiple members of several protein families and complexes: two ATP synthase subunits (ATP5A1 and ATP6V1A), six chaperonins containing T-complex components (CCT2, CCT3, CCT4, CCT5, CCT7, and CCT8), three thioredoxin domain proteins (P4HB, PRDX1, and PRDX2), and four members of the 14-3-3 family (YWHAB, YWHAE, YWHAH, and YWHAQ) (**Figure 2A**).

MCL clustering analysis was performed on the 33 shared proteins using the STRING database, which integrates information from various databases cataloging known and predicted protein-protein interactions. The analysis generated groups called “clusters,” characterized by a higher density of predicted associations within the clusters compared to those between clusters. Notably, 31 out of the 33 proteins formed a single, highly interconnected cluster, suggesting potential functional relationships between them. Two proteins, VAT1 and ALDH1A1, were excluded from this cluster, as there are no predicted interactions between these proteins and the other 31 proteins (**Figure 2B**). These findings are summarized in **Figure 2C.**

Figure 2

A

	WT mouse THIQ eluate	WT mouse Control eluate	SOD mouse THIQ eluate	SOD mouse control eluate	Healthy PBMC 44 THIQ eluate	Healthy PBMC 52 THIQ eluate	ALS PBMC 43 THIQ eluate	ALS PBMC 53 THIQ eluate	ALS PBMC 43 Control eluate	Causitive genes	Associated and disease modifier genes	ALS protein binding partners	KEGG ALS interactome
ACTN4	7	0	4	0	64	69	78	69	0				
ALDH1A1	2	0	7	0	8	0	0	2	0				
ATP5A1	22	0	17	0	2	5	5	6	0				
ATP6V1A	13	0	7	0	3	0	5	0	0				
CALM1	11	0	10	0	13	13	11	12	0				
CCT2	8	0	13	0	7	0	3	0	0				
CCT3	6	0	2	0	8	2	6	2	0				
CCT4	3	0	6	0	8	0	3	2	0				
CCT5	9	0	8	0	9	2	5	0	0				
CCT7	4	0	6	0	8	0	4	0	0				
CCT8	8	0	7	0	11	0	7	2	0				
EEF1G	9	2	10	0	4	4	5	2	0				
HSP90AA1	37	0	44	0	20	13	15	11	0				
HSP90AB1	39	0	46	0	19	15	15	8	0				
HSPA5	11	0	15	0	0	7	0	0	0				
HSPB1	4	0	6	0	4	17	10	0	0				
HSPD1	38	2	38	0	12	21	12	9	0				
LDHB	7	0	0	0	14	0	12	0	0				
P4HB	16	0	23	0	54	48	64	43	0				
PRDX1	8	0	11	0	8	6	4	4	0				
PRDX2	7	0	10	0	18	8	9	19	0				
ST13	6	0	11	0	3	0	4	5	0				
STIP1	32	0	35	0	3	9	0	0	0				
TCP1	6	0	5	0	6	0	4	0	0				
TUBA1A	17	0	15	0	10	12	15	18	0				
TUBA4A	16	3	12	0	11	14	18	18	0				
USP5	12	0	23	0	5	0	2	0	0				
VAT1	9	0	10	0	4	0	10	3	0				
VCP	47	2	53	0	55	62	58	55	0				
YWHAB	9	0	0	0	12	6	9	0	0				
YWHAE	9	0	11	0	6	6	6	0	0				
YWHAH	6	0	7	0	6	7	8	0	0				
YWHAQ	10	0	9	0	0	5	6	7	0				

B

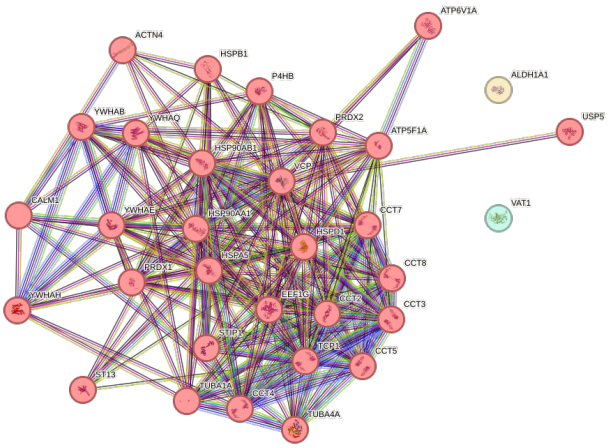

C

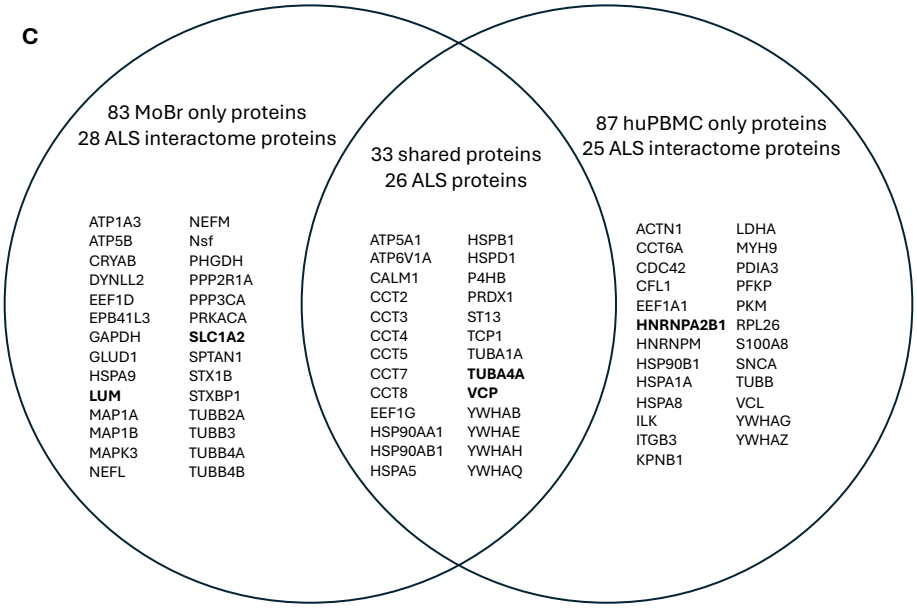

Legend to Figure 2. A**.** Spectral counts for proteins identified in THIQ drug resin eluate from MoBr and human PBMC extracts. Colors represent the number of spectral counts for a given protein in each sample, ranging from light green (low counts) to dark green (high counts). The right panel indicates "hits" for proteins present in the ALS interactome, where yellow is a hit. B. STRING database protein-protein interaction network with MCL clustering. Each circle ("node") represents a protein, and each line

("edge") represents a predicted interaction between two nodes. Different colors represent distinct clusters identified by the MCL algorithm, with red indicating the largest cluster and yellow and green representing clusters containing only a single protein. C. ALS interactome proteins identified by MS-MS are shown in venn diagram. Causative and disease modifier proteins are in **bold**.

From the MS-MS analysis it was clear that the multi-protein complex isolated from PBMCs on the ALS-active drug resin appears related to that observed in MoBr, based on the 27 shared proteins identified that are in the ALS protein interactome observed from both sources. However no clear differences between healthy and ALS patients were observed by MS-MS.

Recognizing that MS-MS analysis as carried out here can fail to identify specific proteins for a number of reasons, including covalent post-translational modifications (PTMs) that alter peptide mass, or result in failure of peptide cleavage with trypsin and/or ionization, we analyzed the DRAC bound material by WB to identify particular proteins of interest. WB has its own limitations, partially but not completely overlapping with those of MS-MS. A shared limitation with MS-MS is that a covalent post-translational can mask an epitope making it undetectable by an epitope-specific antibody. Nevertheless, if a difference between healthy and ALS patients in a protein within the drug resin-bound target complex were identified either by WB or MS-MS, it could serve as a signature of the disease. From WB of the DRAC bound material two proteins were strikingly different between most healthy individuals studied and most ALS patients. First, p62/SQSTM1, a known regulator of autophagy, an important host defensive mechanism, was greatly diminished in ALS patient PBMC DRAC free drug eluates compared to that from most

healthy individuals. Conversely, a 17kDa post-translationally modified fragment of RanGTPase was detected in ALS patients, but not in most healthy individuals, in DRAC free drug eluates. A representative example is shown in Figure 3.

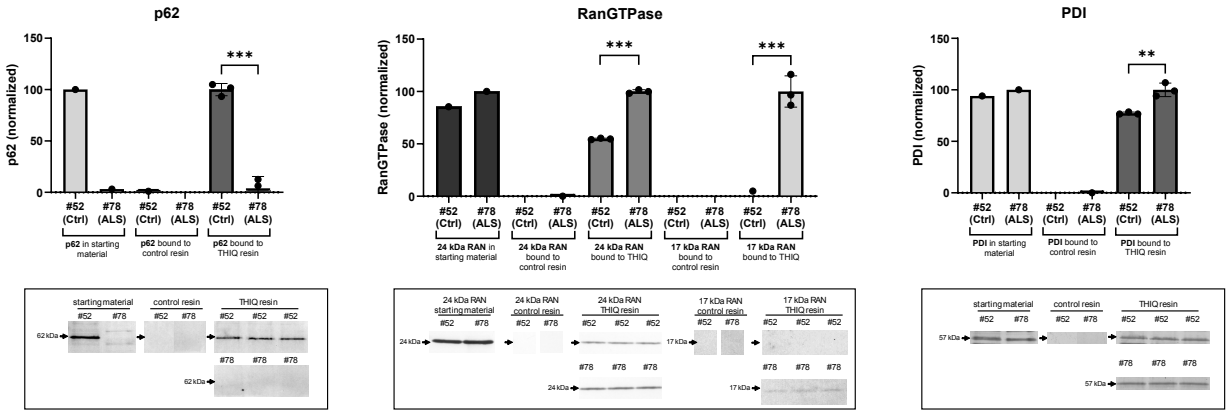

Legend to Figure 3. PBMC extracts were prepared as described in methods and applied to drug resin versus control resin, washed and bound proteins analyzed by SDS-PAGE transferred to 0.2u PVDF membrane and WB for the indicated proteins (below) with quantitation of bands using Image J software (above). Shown is DRAC bound material from a healthy control (#52) and a sporadic ALS patient (#78) analyzed by WB for p62/SQSTM1, RanGTPase, and PDI. The highest value in each healthy/ALS graph pair is normalized to 100% for proportional comparison to the lower value.

Out of 13 ALS patients and 6 healthy controls assessed in a blinded fashion, all 13 ALS patients had a strikingly low values for p62 in the drug resin bound material. Of the 6 healthy controls, 2 were low. For Ran 17 kDa fragment, all 13 ALS patients had a lower value than the parallel reference healthy control. Among the 6 healthy controls, the two with low p62 also had high Ran 17 kDa fragment in the eDRAC bound material. In contrast to striking loss of p62 and

231 appearance of RanGTPase 17kDa fragment, only a modest difference in the direct drug-binding
232 protein, PDI, was observed between ALS patients and healthy controls.
233
234 Thus, taken together, the eDRAC signatures observed appear to have a sensitivity
235 approaching 100% and a specificity of approximately 66% for ALS, albeit from a modest sample
236 size. Further studies are needed to understand how these differences come about and what
237 their significance is to the underlying pathophysiology of ALS. Nevertheless, together with the
238 clinical picture, they suggest a basis for early detection of ALS using as an affinity ligand, a small
239 molecule that is therapeutic for the disease in a diversity of animal models studied[14]. Table 1
240 summarizes these findings together with key demographic features of the individuals studied.

	% p62	% 17kDa Ran Fragment	sex	age at onset	age dx	age at presentation	date of death	disease course	sample date (mo/day/yr)
#52 (healthy)	100 (650)	1 (2)	F			41			7/31/18
#40 (ALS)	71 (462)	5 (12)	M	68	71	72	N/A	LMN predominent - early bulbar/trach slow, progressive course	1/24/19
#50 (ALS)	30 (193)	12 (32)	M	46	47	59	10/21/22	Generalized slowly progressive disease	7/31/18 1/24/19
#51 (ALS)	64 (419)	8 (22)	M	38	39	40	3/1/23	UMN predom generalized disease with bulbar compromise	7/31/18
#68 (ALS)	3 (16)	100 (261)	F	78	79	79	N/A	primary bulbar presentation with mostly UMN features	2/19/19
#54 (ALS)	6 (41)	76 (197)	M	51	52	52	2/5/19	rapidly progressive, bulbar involving disease	8/7/18
#55 (healthy)	10 (63)	86 (224)	F			55			
#52 (healthy)	100 (645)	0 (0)	F			41			7/31/18
#45 (ALS)	13 (64)	61 (63)	M	42	43	43	N/A		5/22/18 2/28/19
#78 (ALS)	6 (35)	100 (103)	F	45	46	46	10/7/20	LMN predom, generalized disease	5/28/19 7/18/19
#52 (healthy)	125 (700)	8 (8)	F			41			7/31/18
#87 (healthy)	126 (706)	5 (5)	M			36			12/19/19
#52 (healthy)	100 (710)	0 (0)	F			41			7/31/18
#43 (ALS)	12 (85)	100 (44)	F	68	71	72	12/19/18	UMN predominent; generalized disesease with significant bulbar compromise	12/19/18
#44 (healthy)	15 (105)	27 (12)	F			74			
#46 (ALS)	54 (385)	11 (5)	M	53	54	54	N/A	bulbar onset then generalized disease	5/23/18
#47 (healthy)	56 (400)	7 (3)	M			58			
#53 (ALS)	0 (0)	68 (30)	F	67	68	71	2/12/19	limb onset generalized disease, possible concurrent Parkinson's disease	7/31/18
#26 (healthy)	100 (558)	0 (0)	M			64			1/22/18
#34 (ALS)	1 (3)	7 (2)	M	40	42	42	N/A	monomelic prewesntation VERY slow LMN generalization, bulbar sparing	2/15/18
#69 (ALS)	2 (13)	100 (24)	M	80	82	82	5/8/21	LMN predominant, generalized disease	2/19/19
#70 (ALS)	13 (71)	7 (2)	M	42	42	43	N/A	generalized progressive disease	2/28/19

Legend to Table 1. 13 ALS patients and 6 healthy controls were analyzed over 4 separate experiments and the data tabulated, together with key demographic and clinical history information. For each experiment the highest value p62 was set at 100% and the others scaled proportionally. Likewise, in each experiment the highest value 17kDa Ran fragment was set at 100% and the others scaled proportionally. The quantified WB band value is also shown in parentheses. Healthy individuals are noted in green, and ALS patients in red, except for the two healthy individuals displaying the ALS phenotype, whose values are in black.

Next, photocrosslinking was carried out with PBMC extracts to which was added a drug analog in which the attachment to resin was replaced by attachment to a biotin and diazirine

251 moiety such that exposure to UV light results in a covalent linkage to the drug binding

252 protein(s). Under native conditions associated proteins of the entire multi-protein complex can

253 be precipitated with streptavidin beads. If the sample is first denatured, then only the direct

254 drug-binding protein will be precipitated with streptavidin beads under the conditions

255 described. Figure 4 demonstrates that PDI is the direct drug-binding protein. It should be noted

256 that P4HB found by MS-MS is the gene name for a member of the PDI family of proteins.

257

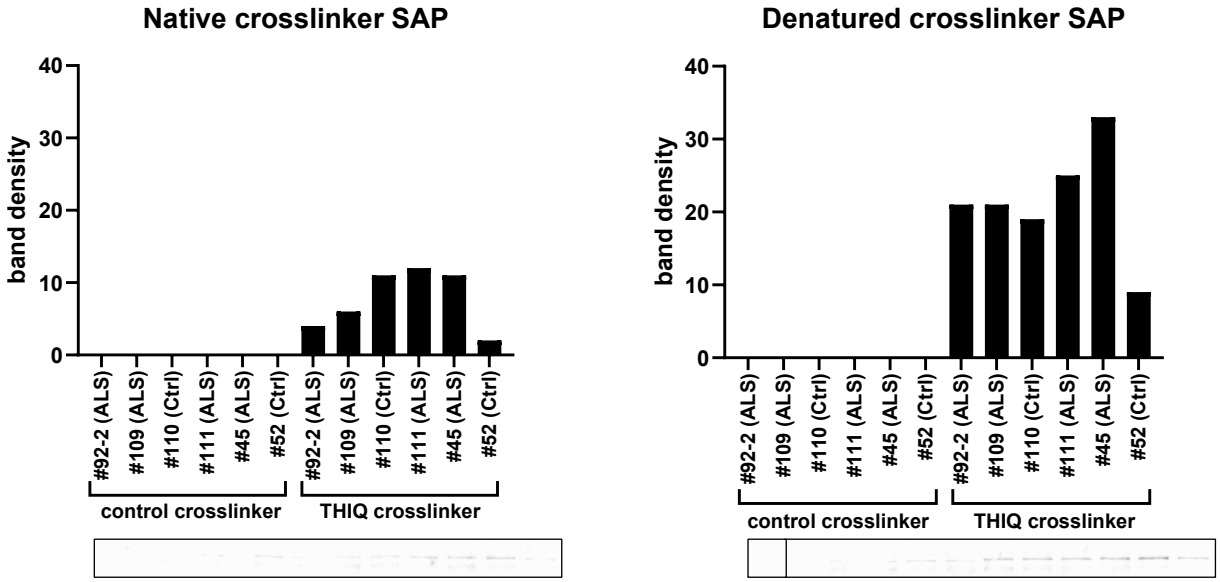

258

259

260 Legend to Figure 4. Quantitation of PDI in streptavidin precipitates under native vs denatured

261 conditions after photocrosslinking with PAV-073 analog (THIQ) or control crosslinker lacking the

262 drug ligand. Both control and THIQ crosslinkers contain biotin and diazirine as described in

263 methods and previously[31].

264

265

266 We then assessed whether the ALS patient vs healthy control correlations involving p62
267 and Ran 17kDa fragment, as shown in Figure 3 and Table 1, were accentuated over time with
268 progression of ALS. As can be seen in Figure 5, with progression of disease, the amount of PBMC
269 p62 bound to the resin, which is much higher in healthy individuals (panel A), diminishes with
270 advancement of ALS. In parallel, the amount of the RanGTPase 17kDa fragment, which is
271 missing in PBMCs from healthy individuals, increases with ALS disease progression.
272
273 Notably, the diagnosis of ALS was made in pt 78 very early in her disease progression.
274 She was able to drive herself to the clinic and walk in with a cane, at the time that the initial
275 blood sample was taken, which nevertheless revealed the dual signatures of falling p62 and
276 appearance of Ran 17kDa fragment, in contrast to parallel analysis of a healthy control. As will
277 be seen these features appear to be exacerbated with disease progression.
278 Figure 5.

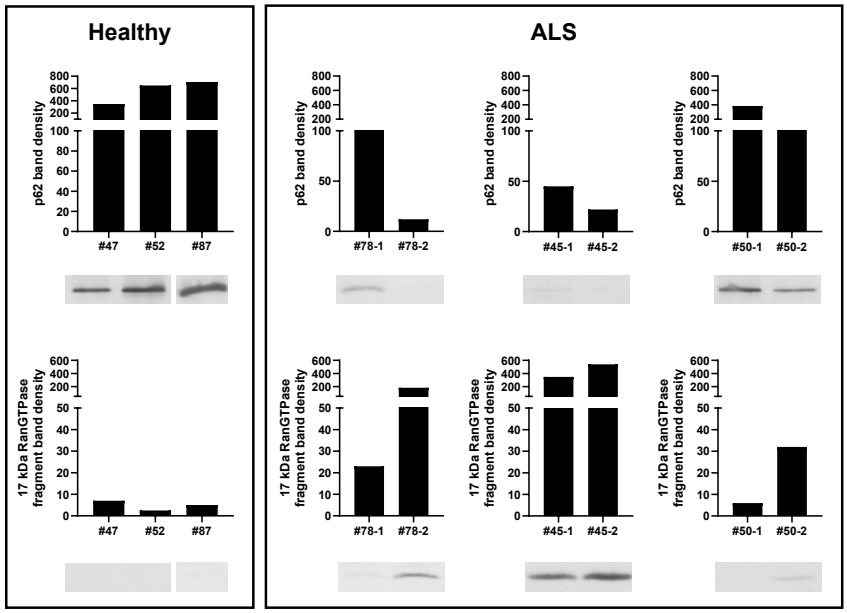

Legend to Figure 5. PBMC extracts were prepared as previously, applied to drug resins and bound proteins analyzed by WB for specific proteins of interest. Bands corresponding to the correct molecular weights were quantified. Blood samples from three ALS patients were assessed over time for both p62 and RanGTPase 17kDa fragment bound to DRAC. Timing of blood draws were 6 weeks apart for patient 78, 6 months apart for patient 50, and 9 months apart for patient 45.

279
280

281 If, as we suggest, ALS represents a breakdown in homeostasis where protective
282 mechanisms to reboot a cellular operating system are ineffective, certain predictions follow. For
283 one, there may be a backup mechanism activated in an attempt to correct the failure of the first
284 line of defense, although by definition, in patients who progress to ALS, that backup has failed
285 to correct the problem. By analogy, when your computer is frozen (with appearance of the
286 "colored wheel of doom"), simply attempting to undo the key stroke that caused it to freeze will
287 not be effective. Instead, it is necessary to reboot the operating system. Perhaps assembly
288 modulators provide precisely such a biochemical reboot of the cellular operating system. In
289 view of the distinctive ALS-associated appearance of a 17kDa fragment of RanGTPase, as noted
290 in Figure 5 above, degradation of RanGTPase, seemed like a plausible backup feedback
291 response. This backup feedback response would be engaged if less draconian feedback methods
292 failed.
293
294 A second prediction is that if, as we hypothesize, assembly modulation is a fundamental
295 mechanism of regulation of gene expression, and its activation by these compounds is
296 therapeutic for ALS, treatment of whole blood from ALS patients with the drugs should result in
297 cessation of the backup RanGTPase degradation feedback loop, upon "reboot" of homeostatic
298 control.
299
300 To test these hypotheses, we took blinded blood samples from ALS patients and healthy
301 controls and treated the whole blood with two different, structurally unrelated ALS therapeutic
302 assembly modulator compounds versus vehicle control (DMSO), and assess the impact after

303 72hrs of incubation (Figure 6). In some samples, RanGTPase was observed to be stable over the

304 course of a 1 hour incubation. These proved to be the healthy controls, when unblinded.

305 However in blood from all of the ALS patients, the levels of RanGTPase after the 1hr incubation

306 were greatly diminished, consistent with what would be expected for degradation of all

307 RanGTPase as an extreme feedback response to the progression of ALS (Figure 6). Upon

308 treatment with either of advanced analogs of two ALS assembly modulator chemotypes (called

309 073 and 667) for 72hrs, a striking diminution of RanGTPase degradation on subsequent 1hr

310 extract incubation was observed, with no change in the level of RanGTPase observed in healthy

311 subjects.

312 Figure 6

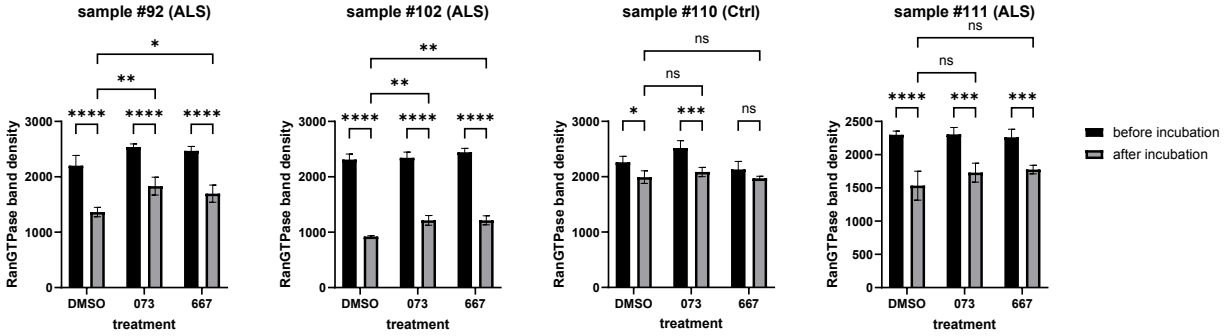

313

314 Legend to Figure 6. 10mls of whole blood from ALS patients or healthy controls was collected under an

315 IRB-approved protocol and shipped overnight at room temperature in EDTA-anticoagulated (purple top)

316 tubes without any patient-specific confidential information. An aliquot of whole blood was taken,

317 incubated in 1% SDS for one hour at 37°C, prepared for SDS-PAGE, and set aside. Another aliquot of

318 whole blood was mixed 1:1 with glucose-supplemented MEM and incubated for 72hrs at 37°C in the

319 presence of vehicle or protein assembly modulator drugs 073 and 667 , at the end of which samples

320 were processed as previously described, and analyzed by SDS-PAGE. Black bars refer to the sample

321 prepared for SDS-PAGE immediately, while gray bars refer to the samples incubated prior to preparation

322 for SDS-PAGE.

323 **Table 2**

Analog representative of chemotype	Molecular weight (g/mol)	log P	H-bond donors	H-bond acceptors	Topological polar surface area (Å²)	Tanimoto similarity coefficient
PAV-073	443.543	4.8	1	5	49	<20%
PAV-667	441.915	6.4	0	7	73.7	<20%

324

Legend to Table 2. Two structurally unrelated (Tanimoto similarity coefficient <20 %) assembly modulator chemotypes used in the experiments shown in Figure 6 are compared for drug-like properties.

325

326 **Discussion**

327 The studies presented here demonstrate the presence, by energy-dependent DRAC and

328 photocrosslinking, of a multi-protein complex in PBMCs that is related to that observed

329 previously by the same method in Tg ALS SOD G93A model MoBr and ALS patient-derived

330 fibroblasts (PDFs) that display both TDP-43 mislocalization and stress-induced agregation[14]. As

331 observed previously for the drug target in MoBr and PDFs, the multi-protein complex drug

332 target in PBMCs has a small subset of PDI as the direct drug-binding protein. The complex

333 present in ALS patient PBMCs also shares with the target in MoBr the presence of 26 proteins

334 implicated in the ALS interactome (Figure 2C). The precise role of this multi-protein complex

335 drug target in ALS pathophysiology remains to be determined. However, based on the efficacy

336 of structurally unrelated ALS assembly modulators in various cellular and animal models, we

337 hypothesize that the drug target serves a role in maintenance of homeostasis, whose loss

338 results in ALS. The presence of p62 in the complex in PBMCs from healthy individuals, and its

339 striking diminution in ALS patient PBMCs, exacerbated with disease progression (Figure 5), are
340 consistent with this hypothesis.
341
342 Likewise, the appearance of a 17kDa post-translationally modified form of RanGTPase in
343 the drug target isolated from ALS patient PBMCs (Figure 3 and Table 1) suggests a complex
344 biology connected to TDP-43 mislocalization, in view of the crucial role of RanGTPase in nucleo-
345 cytoplasmic transport. These changes appear very early in ALS, as suggested by their detection
346 in patient #78 prior to onset of significant disability (Figure 4). In the three cases where a
347 second sample was assessed 6 weeks to 9 months after the first blood draw, both signatures
348 were exacerbated with disease progression. These signatures had a sensitivity of 100%,
349 detected in PBMCs of all 13 sporadic ALS patients studied, and a specificity of 66% for
350 distinguishing ALS patients from healthy individuals. While a larger number of cases will need to
351 be assessed, this early degree of discrimination, using as an affinity ligand a drug shown
352 therapeutically active in a diversity of animal models, is promising as a novel path to an ALS
353 biomarker and highly relevant to ALS therapeutics.
354
355 This target multi-protein complex is implicated in ALS for four reasons. First, the drug
356 that served as the ligand to bind and isolate the target is therapeutic in a wide range of ALS
357 cellular and animal models[31]. Second, the composition of the target multi-protein complex
358 includes a number of proteins of the ALS interactome, 26 of which are shared with the
359 corresponding complex in MoBr. Third, the isolated target from ALS patient PBMCs is altered in
360 protein composition compared to that from most healthy controls by two metrics: diminution of

361 p62/SQSTM1 and appearance of 17kDa fragment of Ran GTPase. Finally, separate from the
362 specific target in PBMCs, a profound degradation of total RanGTPase is observed in whole blood
363 from ALS patients but not in healthy controls, and is substantially rescued after 72hrs of
364 treatment with ALS-active assembly modulators.
365
366 We interpret these findings to suggest that ALS is, fundamentally, a disease of disrupted
367 homeostasis for which assembly modulators may be therapeutic. Looking to other therapeutic
368 areas, it is notable that the vast majority of individuals don't have cancer for most of their lives.
369 However, a small number will develop cancer, at least in part due to failure of homeostatic host
370 defenses. So also host defenses protect most of us most of the time from the consequences of
371 various central nervous system insults, including those causing ALS. Host defenses including
372 restoration of homeostasis, likely allow usually resolution of a CNS insult. Sometimes however,
373 those host defenses appear to fail. As a result, homeostasis is not restored, and progression to
374 motor neuron death is accelerated, culminating in ALS. Presumably more and more severe
375 feedback mechanisms are activated in the course of disease progression, in ongoing futile
376 attempts to restore homeostasis.
377
378 Autophagy, in part mediated by p62/SQSTM1, is an example of a biochemical reboot of
379 the cellular operating system. But what happens when the reboot fails, e.g. due to loss of p62
380 from the dysfunctional target? We propose the consequence, in a range of specific but relatively
381 rare circumstances, is ALS. This persistent deviation from homeostasis is a stress to which
382 motor neurons appear highly sensitive, and eventually, succumb. A drug capable of restoring

383 homeostasis is likely most effective before motor neurons have died, although perhaps synaptic
384 plasticity could synergize allowing some degree of recovery even later, once homeostasis has
385 been restored. Regardless, it is surely a truism of medicine that the earlier a disease is detected,
386 the more effective most therapeutic interventions are likely to be. Hence the importance of
387 early detection to enable early treatment, which the PBMC signatures noted here may provide.
388
389 The results of the whole blood experiments (Figure 6) are consistent with the hypothesis
390 that the degradation of total RanGTPase observed, is an extreme feedback response to the
391 inability more proximal feedback loops to restore the target complex with its small subset of
392 RanGTPase, back to the healthy state. Treatment with either of two structurally unrelated
393 assembly modulators results in correction of the RanGTPase degradation observed in whole
394 blood, to a significant extent. We hypothesize that treatment for a longer period would have
395 completely restored RanGTPase levels to normal. Whether assembly modulator drug treatment
396 serves to fully reboot the system, e.g. restore p62 to the target complex as has been observed
397 for assembly modulation using a structurally unrelated molecule in a different therapeutic
398 area[15], remains to be determined and may vary on a case-by-case basis. Likewise, further
399 studies are needed to determine whether periodic or ongoing drug treatment are required.
400 Regardless, drug-induced changes in target composition, as implied by stabilization of
401 RanGTPase in ALS patient blood treated with assembly modulators, is consistent with
402 restoration of homeostasis. Whether this is reflective of concomitant changes in motor neurons
403 that prevent further motor neuron loss, remains to be investigated.
404

405 Our findings are significant for a number of reasons. First, these studies provide a
406 window into novel regulatory feedback loops involved in cellular homeostasis. The precise
407 relationship of the target multi-protein complex in healthy individuals vs ALS patients remains to
408 be more fully understood. One hypothesis is that the target multi-protein complex in healthy
409 individuals is the "normal" assembly machine involved in integration of diverse events of
410 homeostasis. This includes TDP-43 localization, in which RanGTPase likely plays a critical role,
411 perhaps along with C9orf72 and other ALS-implicated gene products. Other relevant pathways
412 including autophagic removal of dysfunctional multi-protein complexes are naturally integrated
413 into the physiological feedback pathways that collectively bring about homeostasis. ALS may be
414 an example where a "stuck" pathway triggers more and more desperate feedback attempts to
415 reboot the system without success, culminating in the mass degradation of RanGTPase
416 observed in the whole blood experiment shown in Figure 6. In this model, the assembly
417 modulator compound action can be thought of as rebooting the cellular operating system. A
418 future prediction to be tested, is that longer-term treatment of blood results in complete
419 normalization of RanGTPase – and restoration of p62/SQSTM1 -- in the target complex present
420 in PBMCs. By virtue of having therapeutic small molecules as affinity ligands for target
421 identification, the pathways discovered can be productively illuminated by future studies,
422 including by fractionation and reconstitution of functional activities in extracts.
423
424 Second, these data, together with the studies shown previously, are consistent with the
425 hypothesis that, despite the heterogeneity of ALS clinical presentation and time course of
426 progression, there is a common underlying pathway that is the basis of the disease – and that

427 assembly modulators are therapeutic at that underlying shared level. While we hypothesize that
428 restoration of autophagy is a crucial part of this pathway, re-establishment of homeostasis likely
429 involves far more than just restoration of autophagy. In this regards the involvement of
430 miniscule subsets of the specific gene products found together in the target multi-protein
431 complex and the role of protein degradation, is notable. These targets could not have been
432 detected by powerful molecular biological tools such as CRISPR or siRNA knockdown studies,
433 because of the heterogeneous roles of small subsets of many, if not most, of the proteins
434 comprising the target multi-protein complex. Thus the concept of protein "moonlighting"[34,35]
435 may be more pervasive than is currently generally recognized. Conversely, the level of
436 organization of gene expression accessed by protein assembly modulation may be therapeutic
437 for diverse diseases in ways not generally appreciated today.
438
439 Finally, it should be noted that many if not most patients come to medical attention long
440 after the most effective period of treatment is lost. Drugs to stop the disease process may still
441 be effective, but rely on maintenance of the underlying framework of feedback loops to restore
442 homeostasis, once disease progression is arrested. Sometimes however, those feedback loops
443 fail and homeostasis is not restored, whether or not the primary disease process has been
444 blocked. We hypothesize ALS is one such example, making it extremely difficult to treat. The
445 methods described here provide a means of detecting ALS early, prior to onset of severe
446 disability, when it is most treatable – and provide a potentially effective treatment in the form
447 of the small molecule ligands themselves, that were used for disease detection. It is notable
448 that pt 78 came to medical attention early in her clinical course, prior to serious disability, and

449 yet, the signature changes (lowered p62 and elevated RanGTPase 17kDa fragment) were
450 nevertheless observed, and sadly, progressed with worsening of ALS, culminating in her death,
451 approximately 2 years after initial detection of the Ran 17kDa fragment as shown in Figure 5,
452 together with the reciprocal change in p62/SQSTM1, seen exacerbated over time. To date, these
453 findings have been observed in 13 of 13 ALS patients and are lacking in 4 of 6 healthy controls,
454 by the methods described. While the specificity of these signatures are relatively low, seen in 2
455 of 6 healthy controls, the high sensitivity implied by detection in 13 of 13 ALS patients, together
456 with the clinical history, make this diagnostic approach promising. PBMCs are a readily
457 accessible tissue. Used as affinity ligands, these small molecules could enable early diagnosis of
458 ALS, prior to extensive motor neuron death, when treatment would be more effective.
459 Remarkably, these same small molecules may ultimately prove therapeutic, particularly for ALS
460 detected early, by virtue of this peripheral blood signature.
461

462 **Methods**

463 **Preparation of PBMC extracts**[36]

464 Whole blood collected in purple-top EDTA tubes from healthy individuals or ALS patients under
465 Loma Linda Medical Center IRB# 5160136 was shipped by overnight courier to the lab where it
466 was diluted 1:1 with phosphate-buffered saline and layered on ficoll and centrifuged for 15
467 minutes at 1,000 xg at room temperature with brake off. PBMCs were collected at the
468 interface, diluted with PBS 1:1 and centrifuged at 600 xg /15 minutes. The supernatant was
469 aspirated and the pellet dissolved in p-body buffer (PBB) consisting of 10mM Tris pH 7.5 ,10mM

470 NaCl, 6mM MgAc, 1mM EDTA, and 0.35% Triton-X-100 and centrifuged at 4oC 10,000xg/10min.
471 The 10kxg supernate was collected, aliquoted and flash frozen in liquid nitrogen and stored at
472 -80°C until use.
473

474 **Assembly modulator compounds**

475 Each assembly modulator chemotype is structurally quite different from one another,
476 depending on the target to which it is directed, the allosteric site involved, etc. The two ALS-
477 active assembly modulator chemotypes used here, typified by compounds PAV-073 and PAV-
478 667 are compared for drug-like properties in Table 2. The structure of PAV-073, a member of
479 the THIQ chemotype, its synthesis and modification to allow its use as an affinity ligand for drug
480 resin affinity chromatography is described in reference 14.
481

482 **Drug Resin affinity chromatography**

483 A variation on the theme of methods described in previous publications[14–16]. For
484 brain from wildtype or SOD1 mutant animals, tissue was homogenized in cold low salt buffer
485 (10mM HEPES pH 7.6, 10mM NaCl, 1mM MgAc with 0.35% Tritonx100) then centrifuged at
486 10,000 xg for 10 minutes at 4°C. The post-mitochondrial supernatant was adjusted to a
487 concentration of approximately 10 mg/ml and equiulibrated in a physiologic column buffer (50
488 mM Hepes ph 7.6, 100 mM KAc, 6 mM MgAc, 1 mM EDTA, 4mM TGA). For DRAC of both MoBr

489 and human PBMC extracts, the 10k sup samples being compared were first normalized either by
490 absorbance at 280nm or by Coomassie brilliant blue or silver staining pattern. Samples were
491 then supplemented with an energy cocktail (to a final concentration of 1mM rATP, 1mM rGTP,
492 1mM rCTP, 1mM rUTP, and 5 µg/mL creatine kinase) in the presence of physiological salts
493 (50mM Hepes pH 7.6, 100mM Kac, MgAc 5mM, 1mM DTT) and incubated for one hour at either
494 4° C or 22° C degrees on 30 µl of affigel resin coupled to THIQ compound or a 4% agarose matrix
495 (control). The input material was collected after flow through the column and the resin was
496 then washed with 3 ml column buffer. The resins were eluted for 2 hours then overnight at 22°C
497 then 4°C in 100µl column buffer containing 100µM of the cognate compound. Eluates were run
498 on WB or sent for MS-MS for analysis.
499
500 **Chemical photocrosslinking**
501 A variation of protocols as published previously[14] was used. Extract from MoBr were prepared
502 as described above then adjusted to a protein concentration of approximately 3 mg/ml in
503 column buffer (Hepes pH 7.5 50mM, Kac 100mM, MgAc 5mM, DTT or TGA 1mM) containing
504 0.1% triton. 1% DMSO or 100µM PAV-073 was added to 6µl of extract, then 3µM of PAV-073
505 photocrosslinker or a negative control crosslinker (comprising of the biotin and diazirine
506 moieties without compound) were added. The extract was incubated for 20 minutes then
507 exposed to UV at 365nM wavelength for 10 minutes then left on ice for one hour. After
508 crosslinking, samples were divided in two 20 µl aliquots and one set was denatured by adding
509 20 µL of column buffer 4µl of 10% SDS, 0.5 µl 1M dithiothreitol (DTT), and heating to 100°C for 5
510 minutes. Both native and denatured aliquots were then diluted in 800 µl column buffer

511 containing 0.1% triton. 5 µl of magnetic streptavidin beads (Pierce) were added to all samples
512 and mixed for one hour at room temperature to capture all biotinylated proteins and co-
513 associated proteins. Samples were placed on a magnetic rack to hold the beads in placed and
514 washed three times with 800 µl of column buffer containing 0.1% triton. After washing, beads
515 were resuspended in 80 µl of gel loading buffer containing SDS and analyzed by WB or blot for
516 affinity purified streptavidin. Samples were analyzed by WB
517
518 **WB Procedure**
519 SDS-PAGE gels were transferred in Towbin buffer (25mM Tris, 192mM glycine, 20% w/v
520 methanol) to polyvinylidene fluoride membrane, blocked in 1% bovine serum albumin (BSA) in
521 PBS, incubated overnight at 4°C in a 1:1 dilution of 100µg/mL affinity-purified primary rabbit
522 IGG to PDI (Abcam 96744) in 1% BSA in PBS containing 0.1% Tween-20 (PBST). Membranes were
523 then washed twice in PBST and incubated for two hours at room temperature in a 1:5,000
524 dilution of secondary anti-rabbit or anti-mouse antibody coupled to alkaline phosphatase in
525 PBST. Membranes were washed two more times in PBST then incubated in a developer solution
526 prepared from 100 µL of 7.5 mg/mL 5-bromo-4-chloro-3-indolyl phosphate dissolved in 60%
527 dimethyl formamide (DMF) in water and 100µl of 15 mg/ml nitro blue tetrazolium dissolved in
528 70% DMF in water, adjusted to 50mL with 0.1 Tris (pH 9.5) and 0.1 mM magnesium chloride.
529 Membranes were scanned and the integrated density of protein band was measured on ImageJ.
530 Averages and the standard deviation between repeated experiments were calculated and
531 plotted on Microsoft Excel. Primary antibodies for RanGTPase (Abcam ab31118), p62/SQSTM1

532 (Abcam, ab56416), were used at 1:1,000 dilution by the same procedure. Secondary goat
533 antibodies to mouse (Abcam ab97020) or rabbit (Abcam ab6722) were used at 1:5,000 dilution.
534
535 **Tandem mass spectrometry**
536 Samples were processed by SDS PAGE using a 10% Bis-tris NuPAGE gel with the 2-(N-
537 morpholino)ethanesulfonic acid buffer system. The mobility region, including all proteins, was
538 excised and washed with 25 mM ammonium bicarbonate followed by 15mM acetonitrile.
539 Samples were reduced with 10 mM dithoithreitol and 60° C followed by alkylation with 50 mM
540 iodoacetamide at room temperature. Samples were then digested with trypsin (Promega)
541 overnight (18 hours) at 37° C then quenched with formic acid and desalted using an Empore SD
542 plate. Half of each digested sample was analyzed by LC-MS/MS with a Waters NanoAcquity
543 HPLC system interfaced to a ThermoFisher Q Exactive. Peptides were loaded on a trapping
544 column and eluted over a 75 µM analytical column at 350 nL/min packed with Luna C18 resin
545 (Phenomenex). The mass spectrometer was operated in a data dependent mode, with the
546 Oribtrap operating at 60,000 FWHM and 15,000 FWHM for MS and MS/MS respectively. The
547 fifteen most abundant ions were selected for MS/MS.
548
549 Data was searched using a local copy of Mascot (Matrix Science) with the following parameters:
550 Enzyme: Trypsin/P; Database: SwissProt Human (conducted forward and reverse plus common
551 contaminants); Fixed modification: Carbamidomethyl (C) Variable modifications: Oxidation (M),
552 Acetyl (N-term), Pyro-Glu (N-term Q), Deamidation (N/Q) Mass values: Monoisotopic; Peptide

553 Mass Tolerance: 10 ppm; Fragment Mass Tolerance: 0.02 Da; Max Missed Cleavages: 2. The data
554 was analyzed by spectral count methods.
555
556 **Whole blood incubation and analysis**. 100µl aliquots of EDTA-anticoagulated whole blood is dispensed
557 into 24 well plates containing 100µl of room temperature 80% PBS with 10mM glucose and then treated
558 with DMSO to 0.01% or drug in DMSO to the same dilution with final concentration of 5µM drug. After
559 72hrs samples are collected and adjusted to 1% SDS. One aliquot was prepared in gel loading buffer as
560 starting material. Another aliquot added to energy cocktail (1mM rNTPs with 0.2µg/ml CK, 50mM Hepes
561 pH 7.6 100mK KAc, 6mM MgAc and 4mM TGA) at total volume 100µl and incubated at 37°C for 1hr, and
562 then prepared in gel loading buffer. Samples were analyzed by SDS-PAGE and WB for full length
563 RanGTPase.
564
565 **References**

566 1. Al-Chalabi, A. & Hardiman, O. The epidemiology of ALS: a conspiracy of genes, environment
567 and time. *Nat. Rev. Neurol.* **9**, 617–628 (2013).
568 2. Chiò, A. *et al.* Prognostic factors in ALS: A critical review. *Amyotroph. Lateral Scler. Off. Publ.*
569 *World Fed. Neurol. Res. Group Mot. Neuron Dis.* **10**, 310–323 (2009).
570 3. Rizea, R. E., Corlatescu, A.-D., Costin, H. P., Dumitru, A. & Ciurea, A. V. Understanding
571 Amyotrophic Lateral Sclerosis: Pathophysiology, Diagnosis, and Therapeutic Advances. *Int. J.*
572 *Mol. Sci.* **25**, 9966 (2024).
573 4. Hernan-Godoy, M. & Rouaux, C. From Environment to Gene Expression: Epigenetic
574 Methylations and One-Carbon Metabolism in Amyotrophic Lateral Sclerosis. *Cells* **13**, 967
575 (2024).

576 5. Cabrera-Rodríguez, R. *et al.* TDP-43 Controls HIV-1 Viral Production and Virus Infectiveness.
577 *Int. J. Mol. Sci.* **24**, 7658 (2023).
578 6. Gandhi, J. *et al.* Protein misfolding and aggregation in neurodegenerative diseases: a review
579 of pathogeneses, novel detection strategies, and potential therapeutics. *Rev. Neurosci.* **30**,
580 339–358 (2019).
581 7. Grad, L. I., Rouleau, G. A., Ravits, J. & Cashman, N. R. Clinical Spectrum of Amyotrophic
582 Lateral Sclerosis (ALS). *Cold Spring Harb. Perspect. Med.* **7**, (2017).
583 8. Chou, C.-C. *et al.* TDP-43 pathology disrupts nuclear pore complexes and nucleocytoplasmic
584 transport in ALS/FTD. *Nat. Neurosci.* **21**, 228–239 (2018).
585 9. Baradaran-Heravi, Y., Van Broeckhoven, C. & van der Zee, J. Stress granule mediated protein
586 aggregation and underlying gene defects in the FTD-ALS spectrum. *Neurobiol. Dis.* **134**,
587 104639 (2020).
588 10. Gasset-Rosa, F. *et al.* Cytoplasmic TDP-43 De-mixing Independent of Stress Granules Drives
589 Inhibition of Nuclear Import, Loss of Nuclear TDP-43, and Cell Death. *Neuron* **102**, 339-
590 357.e7 (2019).
591 11. Kim, C. K. *et al.* Alzheimer's Disease: Key Insights from Two Decades of Clinical Trial Failures.
592 *J. Alzheimers Dis. JAD* **87**, 83–100 (2022).
593 12. Aggad, D., Vérièpe, J., Tauffenberger, A. & Parker, J. A. TDP-43 toxicity proceeds via calcium
594 dysregulation and necrosis in aging Caenorhabditis elegans motor neurons. *J. Neurosci. Off.*
595 *J. Soc. Neurosci.* **34**, 12093–12103 (2014).
596 13. Buratti, E. & Baralle, F. E. Multiple roles of TDP-43 in gene expression, splicing regulation,
597 and human disease. *Front. Biosci. J. Virtual Libr.* **13**, 867–878 (2008).

14. Yu, S. F. *et al.* Protein Assembly Modulation: A New Approach to Amyotrophic Lateral Sclerosis (ALS) Therapeutics. *J. Exp. Neurol.* **5**, 210–230 (2024).
15. Michon, M. *et al.* A pan-respiratory antiviral chemotype targeting a transient host multi-protein complex. *Open Biol.* **14**, 230363 (2024).
16. Lingappa, A. F. *et al.* Small molecule protein assembly modulators with pan-cancer therapeutic efficacy. *Open Biol.* **14**, 240210 (2024).
17. Bechtel, W. & Bich, L. Situating homeostasis in organisms: maintaining organization through time. *J. Physiol.* **602**, 6003–6020 (2024).
18. Tomkins, G. M. The metabolic code. *Science* **189**, 760–763 (1975).
19. Marty, L. *et al.* The NADPH-dependent thioredoxin system constitutes a functional backup for cytosolic glutathione reductase in Arabidopsis. *Proc. Natl. Acad. Sci. U. S. A.* **106**, 9109–9114 (2009).
20. Noble, D. From Genes to Whole Organs: Connecting Biochemistry to Physiology. in *Novartis Foundation Symposia* (eds. Bock, G. R. & Goode, J. A.) vol. 239 111–128 (Wiley, 2001).
21. Pardee, A. B. Regulatory Molecular Biology. *Cell Cycle* **5**, 846–852 (2006).
22. Pardee, A. B. & Reddy, G. P.-V. Beginnings of feedback inhibition, allostery, and multi-protein complexes. *Gene* **321**, 17–23 (2003).
23. Fenton, A. W. Allostery: an illustrated definition for the 'second secret of life'. *Trends Biochem. Sci.* **33**, 420–425 (2008).
24. Müller-Schiffmann, A. *et al. A Pan-Respiratory Antiviral Chemotype Targeting a Transient Host Multiprotein Complex*. http://biorxiv.org/lookup/doi/10.1101/2021.01.17.426875 (2021) doi:10.1101/2021.01.17.426875.

25. Lingappa, A. F. *et al.* Small Molecule Assembly Modulators with Pan-Cancer Therapeutic Efficacy. *bioRxiv* 2022.09.28.509937 (2022) doi:10.1101/2022.09.28.509937.
26. Nardo, G. *et al.* Amyotrophic lateral sclerosis multiprotein biomarkers in peripheral blood mononuclear cells. *PloS One* **6**, e25545 (2011).
27. Luotti, S. *et al.* Diagnostic and prognostic values of PBMC proteins in amyotrophic lateral sclerosis. *Neurobiol. Dis.* **139**, 104815 (2020).
28. Pongrácová, E., Buratti, E. & Romano, M. Prion-like Spreading of Disease in TDP-43 Proteinopathies. *Brain Sci.* **14**, 1132 (2024).
29. Duyckaerts, C., Clavaguera, F. & Potier, M.-C. The prion-like propagation hypothesis in Alzheimer's and Parkinson's disease. *Curr. Opin. Neurol.* **32**, 266–271 (2019).
30. Wenzhi, Y., Xiangyi, L. & Dongsheng, F. The prion-like effect and prion-like protein targeting strategy in amyotrophic lateral sclerosis. *Heliyon* **10**, e34963 (2024).
31. Feng Yu, S. *et al. Protein Assembly Modulation: A New Approach to ALS Therapeutics*. http://biorxiv.org/lookup/doi/10.1101/2023.07.24.550252 (2023) doi:10.1101/2023.07.24.550252.
32. Dervishi, I. *et al.* Protein-protein interactions reveal key canonical pathways, upstream regulators, interactome domains, and novel targets in ALS. *Sci. Rep.* **8**, 14732 (2018).
33. Kanehisa, M., Furumichi, M., Sato, Y., Kawashima, M. & Ishiguro-Watanabe, M. KEGG for taxonomy-based analysis of pathways and genomes. *Nucleic Acids Res.* **51**, D587–D592 (2023).
34. Copley, S. D. Moonlighting is mainstream: paradigm adjustment required. *BioEssays News Rev. Mol. Cell. Dev. Biol.* **34**, 578–588 (2012).

642 35. Jeffery, C. J. Multitalented actors inside and outside the cell: recent discoveries add to the
643 number of moonlighting proteins. *Biochem. Soc. Trans.* **47**, 1941–1948 (2019).
644 36. Jia, Y. *et al.* A Modified Ficoll-Paque Gradient Method for Isolating Mononuclear Cells from
645 the Peripheral and Umbilical Cord Blood of Humans for Biobanks and Clinical Laboratories.
646 *Biopreservation Biobanking* **16**, 82–91 (2018).
647
648
649
650
651
652
653
654
655

Supplemental Figure 1.

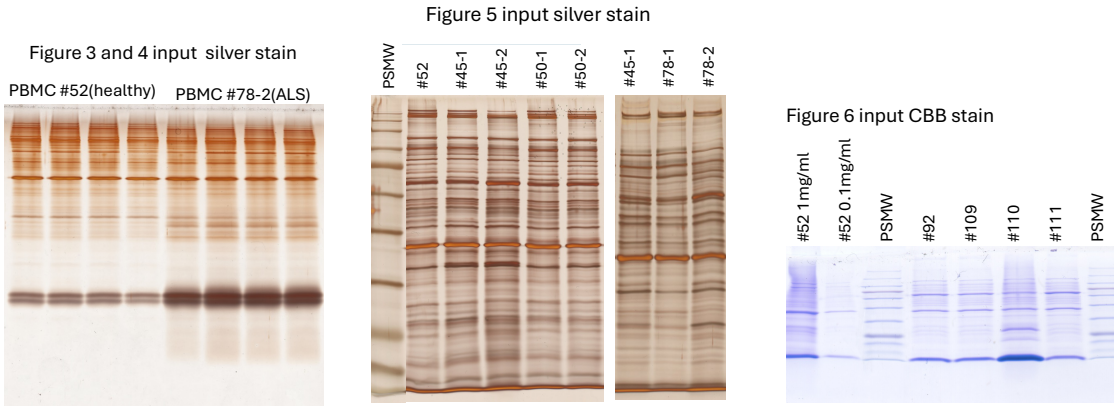

Legend to Supplemental Figure 1. Input extracts for Figures 3-6. Silver stain (left and middle panels) and CBB stain (right panel) of input extracts used for DRAC (Figure 3 and 5), photocrosslinking (Figure 4), and RanGTPase degradation (Figure 6) assays.

656

657

658

659

660

661

662

663

664

665

666

667

668

Supplemental Figure 2

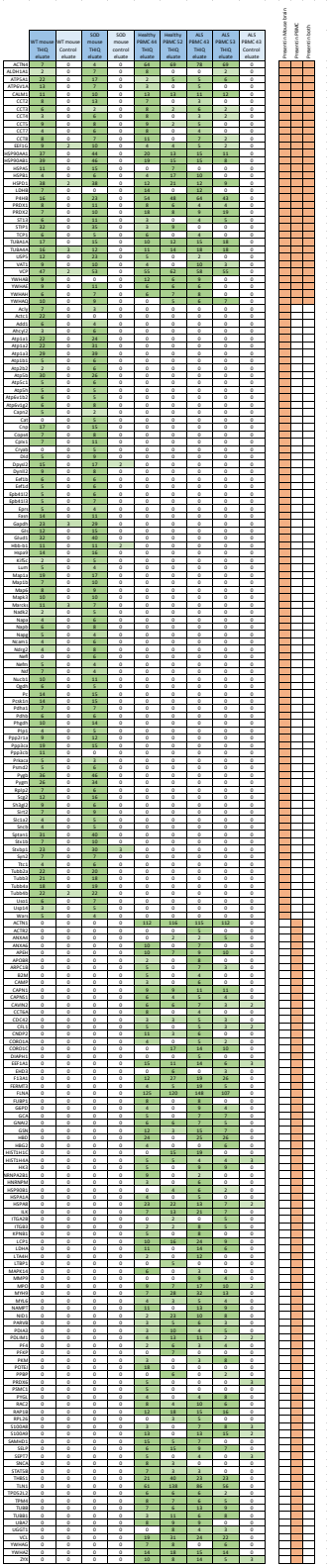

	WT mouse THIQ eluate	WT mouse Control eluate	SOD mouse THIQ eluate	SOD mouse control eluate	healthy PBMC 44 THIQ eluate	healthy PBMC 52 THIQ eluate	ALS PBMC 41 THIQ eluate	ALS PBMC 53 THIQ eluate	ALS PBMC 43 Control eluate
ACTN1	2	0	4	0	54	49	74	69	0
ALDH1A1	2	0	7	0	8	0	0	2	0
ATP1A3	22	0	17	0	2	5	5	8	0
ATP5C1	13	0	7	0	1	0	5	5	0
CALM1	11	0	10	0	13	11	11	12	0
CC72	8	0	13	0	7	4	3	0	0
CC73	6	0	2	0	8	3	6	2	0
CC74	3	0	6	0	8	0	3	2	0
CC75	9	0	8	0	9	3	5	0	0
CC77	4	0	6	0	8	0	4	0	0
CC78	8	0	7	0	11	0	7	2	0
EEF1G	9	2	10	0	4	2	5	2	0
GSPSYAA1	27	0	44	0	20	13	15	11	0
GSPSYAA1	29	0	46	0	19	15	15	8	0
HSPA5	11	0	15	0	0	7	0	0	0
HSPB1	4	0	6	0	0	17	10	0	0
HSPD1	26	2	38	0	12	21	12	0	0
LSM8	7	0	0	0	14	0	12	0	0
PAK4	16	0	22	0	54	49	64	43	0
PRDX1	8	0	11	0	8	6	4	4	0
PRDX2	7	0	10	0	18	9	9	19	0
SC12	6	0	11	0	3	0	4	5	0
STIP1	22	0	35	0	3	0	0	0	0
TCP1	6	0	5	0	6	0	4	0	0
TUBA1A	17	0	15	0	10	12	15	18	0
TUBA4A	16	2	12	0	11	11	18	18	0
UBP5	12	0	23	0	5	0	2	0	0
VIT	9	0	10	0	3	0	10	2	0
YIF2	47	2	53	0	65	67	58	55	0
YWHAB	9	0	0	0	12	6	9	0	0
YWHAE	8	0	13	0	6	5	6	0	0
YWHAG	6	0	7	0	6	4	8	0	0
YWHAZ	10	0	9	0	0	5	6	7	0
Acs1	7	0	3	0	0	0	0	0	0
Acsl1	22	0	0	0	0	0	0	0	0
Ado1	6	0	8	0	0	0	0	0	0
Aha1p2	3	0	6	0	0	0	0	0	0
Atp1a1	22	0	24	0	0	0	0	0	0
Atp1b1	22	0	21	0	0	0	0	0	0
Atp2a3	29	0	39	0	0	0	0	0	0
Atp2b1	5	0	6	0	0	0	0	0	0
Atp2b2	2	0	6	0	0	0	0	0	0
Atp5f1	10	0	24	0	0	0	0	0	0
Atp5h1	5	0	6	0	0	0	0	0	0
Atp5o	5	0	5	0	0	0	0	0	0
Atp6v1e1	6	0	5	0	0	0	0	0	0
Atp6v1g2	6	0	8	0	0	0	0	0	0
Capn2	5	0	7	0	0	0	0	0	0
Car2	9	0	5	0	0	0	0	0	0
Cnp	17	0	15	0	0	0	0	0	0
Copb2	7	0	8	0	0	0	0	0	0
Cpn1	7	0	11	0	0	0	0	0	0
Crip1	0	0	5	0	0	0	0	0	0
Dbi	5	0	9	0	0	0	0	0	0
Dpyd	15	0	17	2	0	0	0	0	0
Dynll2	9	0	8	0	0	0	0	0	0
Eef1b	6	0	6	0	0	0	0	0	0
Eef1d	5	0	6	0	0	0	0	0	0
Eif4a1	5	0	6	0	0	0	0	0	0
Eif4b	5	0	7	0	0	0	0	0	0
Epb41	5	0	4	0	0	0	0	0	0
Fasn	14	0	11	0	0	0	0	0	0
Gapdh	22	2	29	0	0	0	0	0	0
Gc	12	0	15	0	0	0	0	0	0
Ghdh	32	0	40	0	0	0	0	0	0
Hba-b1	11	0	11	2	0	0	0	0	0
Hspa8	14	0	14	0	0	0	0	0	0
Ide	2	0	5	0	0	0	0	0	0
Lum	5	0	4	0	0	0	0	0	0
Map1a	19	0	17	0	0	0	0	0	0
Map1b	7	0	10	0	0	0	0	0	0
Mbp	8	0	8	0	0	0	0	0	0
Mpz	10	0	10	0	0	0	0	0	0
Mycbp	11	0	7	0	0	0	0	0	0
Nadk2	2	0	5	0	0	0	0	0	0
Nap1l	4	0	6	0	0	0	0	0	0
Nap1l5	6	0	8	0	0	0	0	0	0
Nbdy	5	0	4	0	0	0	0	0	0
Ncam1	4	0	6	0	0	0	0	0	0
Ndrg2	4	0	8	0	0	0	0	0	0
Ndr1	0	0	6	0	0	0	0	0	0
Nefm	5	0	4	0	0	0	0	0	0
Npc	7	0	4	0	0	0	0	0	0
Nucb1	10	0	11	0	0	0	0	0	0
Ogdh	6	0	5	0	0	0	0	0	0
Pc	14	0	15	0	0	0	0	0	0
Pcbd1	14	0	15	0	0	0	0	0	0
Pdha1	7	0	7	0	0	0	0	0	0
Pdhb	6	0	6	0	0	0	0	0	0
Pfkpm	10	0	14	0	0	0	0	0	0
Pip5k1c	4	0	5	0	0	0	0	0	0
Ppp2r1a	9	0	12	0	0	0	0	0	0
Ppp3ca	10	0	15	0	0	0	0	0	0
Pppde1p	13	0	0	0	0	0	0	0	0
Prkar1a	5	0	3	0	0	0	0	0	0
Prmt2	5	0	6	0	0	0	0	0	0
Psap	26	0	46	0	0	0	0	0	0
Pygm	24	0	34	0	0	0	0	0	0
Rpia2	7	0	6	0	0	0	0	0	0
Sdc2	12	0	16	0	0	0	0	0	0
Slc1a2	9	0	6	0	0	0	0	0	0
Snx3	7	0	9	0	0	0	0	0	0
Sod1	4	0	5	0	0	0	0	0	0
Sod3	4	0	5	0	0	0	0	0	0
Spna2	21	0	40	0	0	0	0	0	0
Stx1b	7	0	10	0	0	0	0	0	0
Sucla2	23	0	30	1	0	0	0	0	0
Syn2	7	0	7	0	0	0	0	0	0
Tfr1	4	0	6	0	0	0	0	0	0
Tubb2a	22	0	20	0	0	0	0	0	0
Tubb3	21	0	18	0	0	0	0	0	0
Tubb4a	18	0	19	0	0	0	0	0	0
Tubb4b	22	2	22	0	0	0	0	0	0
Uba1	6	0	7	0	0	0	0	0	0
Uqcrh	3	0	5	0	0	0	0	0	0
Vcp	5	0	6	0	0	0	0	0	0
ACTN1	0	0	0	0	112	114	132	132	0
ACTN2	0	0	0	0	0	0	5	0	0
ANXA6	0	0	0	0	0	0	2	0	0
ANXA7	0	0	0	0	10	0	7	0	0
APOE	0	0	0	0	10	0	9	10	0
AKR1B1	0	0	0	0	2	0	8	0	0
ABPC1B	0	0	0	0	5	0	7	2	0
BZW1	0	0	0	0	5	0	4	0	0
CAMP	0	0	0	0	3	0	6	0	0
CAPN1	0	0	0	0	9	0	15	14	0
CAPNS1	0	0	0	0	6	4	5	4	0
CAVIN1	0	0	0	0	6	0	7	3	2
CCT5A	0	0	0	0	8	0	4	0	0
CDC42	0	0	0	0	3	0	5	3	0
CFL1	0	0	0	0	5	0	5	3	2
CNBP2	0	0	0	0	23	0	6	0	0
COBL1	0	0	0	0	4	0	5	2	0
COBW2	0	0	0	0	0	17	14	10	0
DIAPH1	0	0	0	0	0	0	5	0	0
EEF1A1	0	0	0	0	13	11	14	6	3
EIF3I	0	0	0	0	0	3	6	3	0
F13A1	0	0	0	0	17	27	19	24	0
FERMT2	0	0	0	0	4	3	19	5	0
FLNA	0	0	0	0	175	170	149	107	0
FLNB1	0	0	0	0	8	0	8	0	0
GAPD	0	0	0	0	4	0	9	4	0
GCN	0	0	0	0	5	0	7	7	0
GNB2	0	0	0	0	6	4	7	5	0
GSN	0	0	0	0	12	0	10	7	0
HBD	0	0	0	0	24	0	25	26	0
HBG2	0	0	0	0	4	0	6	6	0
HISTH1C	0	0	0	0	0	11	10	0	0
HISTH4A	0	0	0	0	5	0	4	4	0
HLA-E	0	0	0	0	5	0	8	6	0
IQSEC2	0	0	0	0	9	0	2	0	0
LNS1B1	0	0	0	0	3	0	8	0	0
LGP1B1	0	0	0	0	0	0	6	2	0
HSPA1A	0	0	0	0	4	0	5	0	0
HSPA8	0	0	0	0	23	22	13	7	2
ILK	0	0	0	0	7	13	21	7	0
ITGA2B	0	0	0	0	0	2	0	5	0
ITGB3	0	0	0	0	2	2	8	5	0
KPNB1	0	0	0	0	5	0	8	0	0
LCP1	0	0	0	0	10	16	24	8	0
LDHA	0	0	0	0	11	0	14	4	0
LTBP4	0	0	0	0	2	0	10	0	0
MAPK1	0	0	0	0	0	5	0	0	0
MAPK3	0	0	0	0	6	0	3	2	0
MBP	0	0	0	0	0	0	8	6	0
MRC	0	0	0	0	9	7	17	10	2
MYH9	0	0	0	0	7	20	32	13	0
MYL6	0	0	0	0	4	0	5	4	0
NAMPT	0	0	0	0	11	0	10	9	0
NDS1	0	0	0	0	2	23	10	8	0
PABPC4	0	0	0	0	3	0	6	2	0
PDIA6	0	0	0	0	3	10	4	5	0
PDLIM1	0	0	0	0	4	12	13	2	2
PFN1	0	0	0	0	2	0	3	4	0
PFKFB3	0	0	0	0	0	2	0	0	0
PKM	0	0	0	0	3	0	3	8	0
PLCD1	0	0	0	0	18	0	0	0	0
PPBP	0	0	0	0	0	6	0	2	0
PRDX6	0	0	0	0	5	0	0	0	3
PSMC2	0	0	0	0	5	0	0	0	0
PYGL	0	0	0	0	8	0	4	8	0
RAC2	0	0	0	0	8	0	10	6	0
RAP1B	0	0	0	0	12	18	13	14	0
RPL26	0	0	0	0	0	3	5	0	0
S100A9	0	0	0	0	3	0	7	8	3
S100A8	0	0	0	0	13	0	13	15	7
SAMHD1	0	0	0	0	15	3	7	0	0
SELP	0	0	0	0	6	25	9	7	0
SERP1	0	0	0	0	5	0	4	0	3
SNCG	0	0	0	0	8	0	0	0	0
STAT1B	0	0	0	0	7	4	3	0	0
TMB4X	0	0	0	0	21	20	23	23	0
TUBA	0	0	0	0	61	108	86	56	0
TPSD1-2	0	0	0	0	6	9	6	2	0
TPM3	0	0	0	0	8	7	6	5	0
TUBB	0	0	0	0	7	6	13	8	0
TUBB1	0	0	0	0	3	13	6	8	0
UBB2	0	0	0	0	8	9	8	0	0
VGF(7)	0	0	0	0	0	8	4	3	0
VCL	0	0	0	0	19	31	24	22	0
YWHAQ	0	0	0	0	7	8	0	6	0
ZYX	0	0	0	0	10	8	14	5	3

Legend to Supplemental Figure 1. Spectral counts for entire dataset of MoBr and PBMC THIQ resin eluates. Colors represent the number of spectral counts for a given protein in each sample, ranging from light green (low counts) to dark green (high counts). The right panel indicates whether a given protein was in one of both of the datasets, according to threshold values of >4 spectral counts in the drug eluate and <4 spectral counts in the control column eluate.

671

672 **Abbreviations**

673 ALS – Amyotrophic Lateral Sclerosis

674 CBB – Coomassie brilliant blue

675 CFPSA – Cell-free protein synthesis and assembly

676 CNS – Central Nervous System

677 DTT - dithiothreitol

678 DRAC – drug resin affinity chromatography

679 DX - diagnosis

680 eDRAC – energy-dependent drug resin affinity chromatography

681 FTD – Fronto-Temporal Dementia

682 HEPES - 4-(2-hydroxyethyl)-1-piperazineethanesulfonic acid

683 IND – investigational new drug

684 MoBr – mouse brain

685 MS-MS – tandem mass spectrometry

686 PBMC – Peripheral blood mononuclear cell

687 PBS – phosphate-buffered saline

688 PDF – patient-derived fibroblast

689 PDI – protein disulfide isomerase

690 PTM – post-translationally modified

691 PSMW – Prestained molecular weight markers

692 SAP – streptavidin precipitation

693 SDS-PAGE – polyacrylamide gel electrophoresis in sodium dodecyl sulfate

694 TGA – thioglycolic acid

695 WB – western blot

696

697 **Dataset**

698 The relevant dataset has been submitted to the DRYAD database and can be accessed upon publication

699 at the following: DOI: 10.5061/dryad.0rxwdbsbm

700

701 **Competing Interests**

702 VRL is CEO and AFL COO of Prosetta Biosciences

703

704 **Funding Statement**

705 This work was supported by Target ALS (grant# IL-2023-C4-L1), DOD CDMRP (grant #.

706 W81XWH2210721), and Prosetta Biosciences.

707

708

709

710